Central Lancashire Online Knowledge (CLoK)

Title	Vision-Based Remote Sensing Imagery Datasets From Benkovac Landmine Test Site Using An Autonomous Drone For Detecting Landmine Locations
Type	Article
URL	https://clok.uclan.ac.uk/49065/
DOI	10.21227/ptsa-qj43
Date	2023
Citation	Kuru, Kaya and Ansell, Darren (2023) Vision-Based Remote Sensing Imagery Datasets From Benkovac Landmine Test Site Using An Autonomous Drone For Detecting Landmine Locations. IEEE Data Port. pp. 1-10.
Creators	Kuru, Kaya and Ansell, Darren

It is advisable to refer to the publisher's version if you intend to cite from the work. 10.21227/ptsa-qj43

For information about Research at UCLan please go to http://www.uclan.ac.uk/research/

Vision-Based Remote Sensing Imagery Datasets From Benkovac Landmine Test Site Using An Autonomous Drone For Detecting Landmine Locations

Kaya Kuru and Darren Ansell

Abstract—Mapping millions of buried landmines rapidly and removing them cost-effectively is supremely important to avoid their potential risks and ease this labour-intensive task. Deploying uninhabited vehicles equipped with multiple remote sensing modalities seems to be an ideal option for performing this task in a non-invasive fashion. This report provides researchers with vision-based remote sensing imagery datasets obtained from a real landmine field in Croatia that incorporated an autonomous uninhabited aerial vehicle (UAV), the so-called LMUAV. Additionally, the related knowledge regarding the literature survey is presented to guide the researchers properly. More explicitly, two remote sensing modalities, namely, multispectral and long-wave infrared (LWIR) cameras were mounted on an advanced autonomous UAV and datasets were collected from a well-designed field containing various types of landmines. In this report, multispectral imagery and LWIR imagery datasets are presented for researchers who can fuse these datasets using their bespoke applications to increase the probability of detection, decrease the false alarm rate, and most importantly, improve their techniques based on the features of vision-based imagery datasets.

Index Terms—Landmine detection, airborne demining, Aerial-supported detection of landmines, UAV-supported detection of landmines, thermal imaging, multispectral imaging, long-wave infrared.

◆

1 INTRODUCTION

FULLY autonomous and semi-autonomous robotic applications are replacing the human workforce, particularly, for dangerous and labour-intensive tasks. The detection and demining of legacy landmines using a human or animal workforce is tremendously risky and labour-intensive. Between 1999 and 2012, more than 1,000 deminers have been killed or injured while undertaking demining operations [1]. There are around 100 million landmines buried all over the world [2] due to the cheap manufacturing [3] and ease of deployment over large areas. The slow demining process [4], affects 61 states dramatically all around the world [5], mainly Bosnia and Herzegovina, Croatian, Serbia, Montenegro, Cambodia, Afghanistan, Iraq, Libya, Syria and most recently war-ridden west of Azerbaijan. At the end of 2005, Bosnia and Herzegovina claimed that more than 4% of the country was suspected to be contaminated by landmines [6]. Two years after the end of the armed conflict, in 1997, 23% of the Croatian territory was considered mine suspected [6]. In Colombia, one of the most mine-affected countries in the world, 10.413 people are the victims of landmines between 1990 and 2013 [7]. There are more than 35,000 amputees affected by a landmine explosion in Cambodia [1]. 26,000 people are either killed or maimed per year on average [8]

and 80% of this figure are children [5] which provides ample reason to ban the production and use of landmines by no means that we believe. Even with recent efforts to curb their use, 10 mines are placed for every mine removed [9]. The exact locations of buried legacy landmines are unknown and landmines can change their locations slightly based on the characteristics of the land and the period of burial time. Removing millions of landmines using conventional techniques would take more than 1100 years [10] with high costs and potential risks, which will affect these countries drastically in many aspects for the years to come. It is urgent to develop a rapid, safe and cost-efficient landmine detection system.

Accurate navigation over rough terrains is perhaps the major challenge for land-based vehicles even though they are supported with different mechanisms such as wheeled, legged, and dragged robots [11]. Moreover scanning larger terrains using those heavy and slow vehicles takes a long time. Therefore, UAVs suited to covering a large area to ease labour-intensive mine clearance have been deployed by several studies using various detection modalities. Badia *et al.* [3] propose a blimp-based UAV that is equipped with a broadly tuned metal-thin oxide chemo-sensor using a bioinspired detection architecture where the use of trained animals is still one of the most commonly used methods for explosive detection [11]. Julian *et al.* [11] propose a UAV-based system using image processing/recognition for partially buried landmine-like objects.

New landmines contain less or no metals which makes them harder to be detected [1]. In other words, there are

- *K. Kuru is with the School of Engineering and Computing, University of Central Lancashire, Fylde Rd, Preston, Lancashire, PR12HE, UK. E-mail: kkuru@uclan.ac.uk*
- *D. Ansell is with the School of Engineering and Computing, University of Central Lancashire, Fylde Rd, Preston, Lancashire, PR12HE, UK.*

many different types of landmines made from a variety of materials in different sizes such as metal, plastic, wood, glass [12], most of which can not be detected with metal detectors using traditional electromagnetic-induction (EMI) methods. Detecting and clearing legacy landmines using human force or animals is tremendously risky and labour-intensive. Mapping millions of buried landmines rapidly and removing them cost-effectively is supremely important to avoid their potential risks and to ease this labour-intensive task. Deploying uninhabited vehicles equipped with multiple remote sensing modalities seems to be an ideal option for performing this task in a non-invasive fashion. We have deployed autonomous airborne vehicles in various disciplines (e.g., [13], [14], [15], [16], [17], [18], [19]) using multiple remote sensors to increase the efficacy of task performance. There have been several attempts to employ multiple modalities to expedite the landmine detection process safely. Each method employed in these attempts has its advantages and drawbacks. Vision-based remote sensing (VBRS) modalities are gaining popularity to cover the shortcomings of the currently employed off-the-shelf conventional techniques, particularly, to detect landmines on larger fields more rapidly. The VBRS techniques are based on different physical principles, e.g., electromagnetic detection, vapor/buolk detection, and optoelectronic imaging [20]. However, the use of these techniques successfully depends strongly on weather, illumination, environmental conditions, soil type, and chosen parameters in an application accordingly [20]. By exploiting this technology, Asmish *et al.* [21] propose a morphological approach to automatic mine detection using multispectral (multiple wavelengths) sensors with an airborne minefield imaging system. Anderson *et al.* [22] analyses the multispectral images for landmines based on histograms. The detection lies in the difference in the thermal characteristics between the soil and the buried objects [20]. Thanh *et al.* [20] propose a 3-D linear forward thermal model for buried landmines; more explicitly, a finite-difference approximation of generalized solutions to the thermal model is proposed. Among the used technologies, the dynamic thermal IR technique (IR images of the soil surface acquired at multiple time instants) seems to be promising to detect shallowly buried non-metallic landmines and distinguish them from other buried objects based on the difference in the thermal characteristics between the soil and buried objects [23] [20], [23]. In other words, the presence of buried objects affects the heat conduction inside the soil and consequently, the soil temperature on the ground above the objects is often different from that of unperturbed areas; this temperature signature can be measured by an IR imaging system placed above the soil area [23].

Despite a lot of effort being needed to detect landmines using automated remote approaches, the detection and removal of millions of buried landmines have still been in progress by conventional manual metho ds and it would require hundreds of years to demine all these mines completely using these manual methods and the development of landmine detection and removal system in a short period has become an urgent need [2] where their removal is costly, highly time-consuming and extremely dangerous [3]. In this sense, this report provides researchers with vision-based remote sensing imagery datasets obtained from a real landmine field in Croatia that incorporated an autonomous uninhabited aerial vehicle (UAV), the so-called LMUAV. More explicitly, two remote sensing modalities, namely, multispectral and long-wave infrared (LWIR) cameras were mounted on an advanced autonomous UAV and datasets were collected from a well-designed field containing various types of landmines. In this report, multispectral imagery and LWIR imagery datasets are presented for researchers who can fuse these datasets using their bespoke applications to increase the probability of detection, decrease the false alarm rate, and most importantly, improve their techniques based on the features of vision-based imagery datasets.

2 DATA COLLECTION METHODOLOGY

John *et al.* [24], [25] studies on landmine detection using hyperspectral imaging by analysing the spectral wavelengths on surrounding background objects and landmines. Additionally, he *et al.* [26] explores the various processing techniques on spectral images regarding data fusion, spectral unmixing, classification and target detection. After testing several hyperspectral imagers of different bands, it was found that imagers in LWIR bands have the potential to detect buried landmines with the use of proper algorithms [1]. Several supervised and unsupervised techniques applied on spectral images for landmine detection and their results are presented in Rafic's study [27]: the performed virtual experiments show that mines possess spectral features that allow them to be differentiated from other materials.

2.1 Components of the methodology

The features of the primary system components shown in Fig. 1 are explained in Sections 2.1.1, and 2.1.2.

2.1.1 LMUAV

Current sensors onboard airborne and spaceborne platforms cover large areas of the Earth's surface with unprecedented spectral, spatial, and temporal resolutions [26]. Previous tests used an airborne hyperspectral imaging system for landmine detection, mounted on a fixed-wing manned aircraft or a helicopter [4]. However, a high spatial resolution is necessary to perform landmine detection with high accuracy rates. Therefore, it is necessary to test the ability of a multirotor drone to carry the hyperspectral imager [4]. Similarly, the resolution is very poor with the use of GPR mounted on aircraft or a helicopter for landmine detection where they have to fly at a safe altitude above the ground level. Landmine detection with a multirotor drone could be very promising since it allows to detection of high-quality images with few artifacts caused by undesired motions [4] and high-quality underground impedance tomography. Accurate system positioning information is obtained, in real-time, by means of a Global Positioning System (GPS) and Geographic Information Systems (GIS) using an RTK GPS with centimetre (cm) precision. The LMUAV has advanced user-friendly interfaces to specify the routes to follow. The LMUAV can follow these pre-specified routes over uneven terrain and collect data fully automatically with no human intervention until the battery runs out. A routing scheme
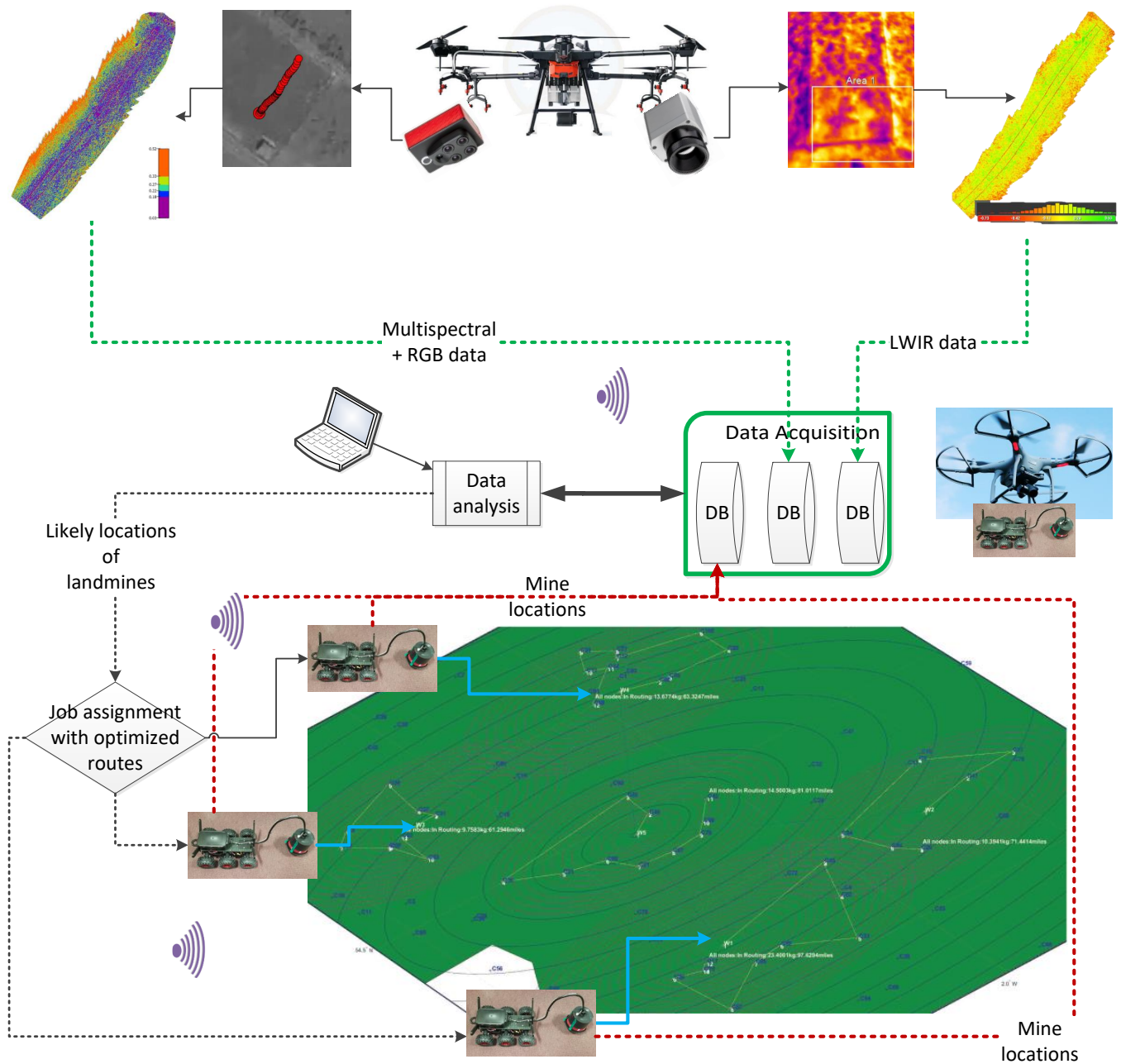
Fig. 1: Overall data collection methodology.

with the LMUAV is displayed in Fig. 2. Humans avoid entering dangerous and harsh topographic minefields by using the LMUAV with automatic missions. Sensor data is recorded onboard using specialized data-acquisition equipment and can be transferred to the ground in real-time using WiFi and Bluetooth connections for real-time data processing. The sensor modalities can be controlled by adjusting the settings from the ground. This integrated system can work robustly in unattended mode using an application that combines data streams acquired from these modalities and autopilot.

2.1.2   Vision-based remote sensing (VBRS) modalities

Thermal inertia is a measure of a material's resistance to temperature fluctuations and is a way to quantify variable responses to temperature change [28]. Landmine burying changes the thermal properties of the upper level of some types of soils and it also changes its surface reflectivity and stresses vegetation [4]. Hence, buried landmines can be detected by measuring the change of reflectivity both between manipulated soil and background and between stressed and unstressed vegetation [4] specifically using unique thermal inertia signatures. The human eye can only respond to wavelengths between roughly 390-700 nm whereas hyperspectral imagers range from 400 to 1000 nm with the invention of Visible and Near-IR (VNIR) [4], which is used in various disciplines such as mapping, agriculture, astronomy, food monitoring and surveillance [1].

The attempts to detect the landmines using spectral imaging can be found in Makki's study [4] in chronolog-

Fig. 2: The route specification interface of the UAV with respect to geospatial map for autonomous use of the UAV.
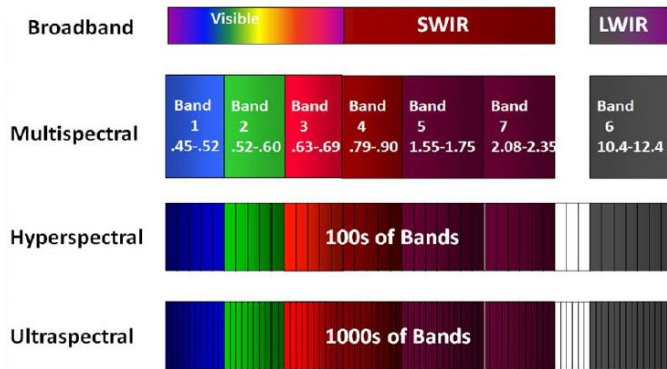

Fig. 3: Frequency bands of spectral imaging [1]

ical order. VNIR (400 to 1000 nm wavelength) spectral signatures are not able to distinguish anthropogenic objects from natural features. Short wave IR (SWIR) bands range from 1 to 2.5 µm and old buried landmines are hard to be detected using SWIR [29]. On the other hand, mid-wave IR (MWIR) is between 3-5 µm whereas LWIR is between 8–12 µm bands [4]. LWIR bands are found to be more effective than MWIR [30]. LWIR spectral regions show the most consistent and highest performance for detecting landmines in various studies [4], [31], [32], [33], [34], [35], [36]. LWIR is a subset of the IR band of the electromagnetic spectrum, covering wavelengths ranging from 8µm to 14µm (8,000 to 14,000nm).

A multispectral camera can capture information that is neither available to the human eyes nor to a typical RGB camera. Multispectral imaging effectively exploits differences among radiation characteristics of artificial targets and

natural surfaces [21]. More explicitly, multispectral imaging exploits the property that each material has its unique spectral signatures and the spectrum of a single pixel in a multispectral image provides information about its constituents and surface of the material [37]. In other words, this imaging technique measures the portion of light reflected in hundreds of wavelengths/frequencies at each image unit (pixel) [1], which obtains a hypercube composed of two spatial dimensions and a third dimension that contains spectral information (i.e., sample x lines x bands). Since different substances heat and cool over the day at different rates, objects in the soil such as landmine cases, ought to show up in this data. In this regard, two main vision-based detectors are employed to help geotag landmines. These detectors specific to our data collection methodology are explored as follows.

Longwave Infrared (LWIR) camera The LWIR camera used for IR sensing, namely Optris PI 640, mounted on the UAV is presented in Fig. 4. Optris PI 640 is the smallest measuring Video Graphics Array (VGA) IR camera worldwide with an optical resolution of 640x480 pixels and is mainly used for temperature measurement using IR in various industry fields. It delivers pin-sharp radiometric pictures and videos in real-time with a body-sized 45x56x90 mm and weighing only 320 grams including the lens. It is among the most compact thermal imaging cameras on the market. The temperature ranges from -20°C to 900 °C. Its spectral ranges from 7.5 to 13 µm with a frame rate of 32Hz [2]. An image

1. https://www.processindustryinformer.com/product-update/powerful-mini-pc-infrared-cameras/

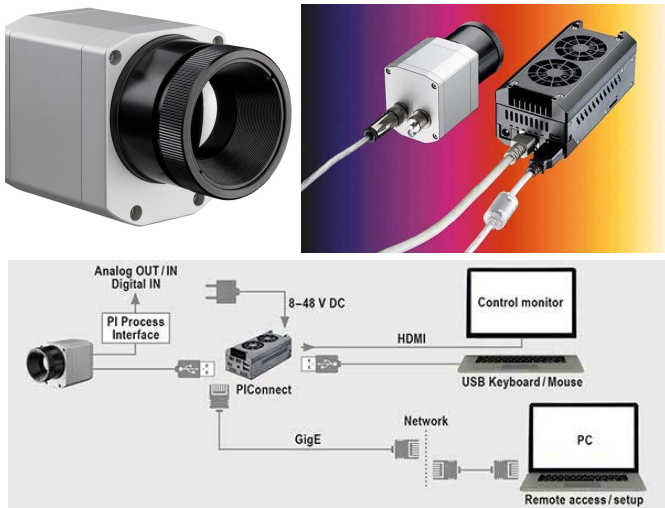2. Interested readers can find more technical information about this camera on https://www.luchsinger.it/contents/products/data-sheet-pi-640.pdf.

Fig. 4: LWIR camera: Optris PI 640[1].

Fig. 5: Multi-spectral RGB camera: Parrot SEQUOIA + multispectral sensor.

from lane-1 using the LWIR camera is depicted in Fig. 7. This camera with its sensors is designed to collect precise image data even under less-than-ideal solar conditions such as cloudy weather conditions. This camera captures the frames and those frames are then combined to establish accurate geospatial imaging using advanced image reconstruction algorithms. This information can be then effectively used to determine the actual imaging geometry and provide crucial information to a particular algorithm to specify the actual locations of landmines.

Multispectral RGB camera The multispectral RGB camera, namely Parrot SEQUOIA+, mounted on the UAV is presented in Fig. 5. Multispectral Parrot SEQUOIA analyses the environment by capturing the amount of light absorbed and reflected with its two sensors, namely multispectral and sunshine. Parrot Sequoia+, combined with Pix4D software is the first multispectral camera to provide absolute reflectance measurements without the need to use radiometric calibration targets. Thanks to Pix4D's new radiometric processing pipeline, Parrot Sequoia+ allows for a more consistent evaluation of collected data and improves the user experience by removing the need for a radiometric calibration target. A full radiometric calibration is automatic when processing data collected using Pix4D software. This will save operational time as well as enable in-depth precision on reflectance measurements. This camera with its sensors is designed to collect precise image data even under less-than-ideal solar conditions as cloudy weather conditions. This camera

TABLE 1: Landmines: lane-1.

x(m)	y(m)	Debt (cm)	Type
2.25	0.85	15	FRAG (saraf)
2.6	0.15	15	ITOP 10
4.55	0.25	15	FRAG (šaraf)
7	0.15	0	PMA 3
7.75	0.3	5	FRAG (šaraf)
8.1	0.95	20	FRAG (saraf)
8.8	0.25	10	Ostatak tromblonske mine
12.55	0.6	10	Ostatak tromblonske mine
13.25	0.25	10	FRAG (saraf)
13.9	0.2	5	PMA 3
14.8	0.35	20	FRAG
15.85	0.3	15	FRAG(saraf)
16.5	0.7	10	FRAG
20.4	0.15	20	FRAG
20.75	0.95	15	FRAG (saraf)
24.2	0.85	20	Bijeli surogat PMA 2
25.4	0.1	20	FRAG (saraf)
26,65	0.6	20	Ostatak tromblonske mine

TABLE 2: Landmines: region-2-.

x(m)	y(m)	Debt(cm)	Type
0.25	0.9	10	Bijeli surogat PMA 2
0.85	0.3	10	FRAG
1.45	0.85	15	PMA 3
2	0.5	10	Plasticcna plava kutija
2.75	0.4	10	PMA 2
3.1	0.95	15	PMA 2
4.2	0.25	10	PMA 2
5.2	0.95	10	PMA 3
6.9	0.45	20	CLUTTER
7.65	0.25	10	PMA 3
8.1	0.9	20	Ostatak tromblonske mine
9.6	0.75	5	PMA 3
10.8	0.3	30	FRAG
12.4	0.4	15	Ostatak tromblonske mine
13.65	0.8	20	Ostatak tromblonske mine
15.25	0.85	20	PMA 2
16.25	0.2	15	FRAG
17.8	0.65	15	puscano zrno
19.9	0.45	20	FRAG
21.25	0.25	10	FRAG
25.2	0.45	20	puscano zrno
26.65	0.65	5	PMA 3
27.3	0.2	5	Bijeli surogat PMA 2
27.3	0.9	5	Bijeli surogat PMA 2
27.7	0.25	10	Bijeli surogat PMA 2
27.7	0.95	5	Bijeli surogat PMA 2
28.05	0.25	10	Bijeli surogat PMA 2
28.05	0.95	10	Bijeli surogat PMA 2
28.45	0.2	10	Bijeli surogat PMA 2
28.45	0.95	10	Bijeli surogat PMA 2
28.85	0.25	10	Bijeli surogat PMA 2
28.85	0.95	5	Bijeli surogat PMA 2
29.35	0.2	20	Bijeli surogat PMA 2
29.35	0.95	5	Bijeli surogat PMA 2

captures the frames and those frames are then combined to establish accurate geospatial imaging using advanced image reconstruction algorithms. This information can be then effectively used to determine the actual imaging geometry and provide crucial information to a particular algorithm to specify the actual geo-locations of landmines.

2.2 Landmine regions

The specific locations of the landmines in 7 regions are presented in Table 1, 2, 3, 4, 5, 6 and 7.

TABLE 3: Landmines: region-3-.

x(m)	y(m)	Depth(cm)	Type
0	0.85	15	Bijeli surogat PMA 2
1.2	0.8	5	PMA 3
1.35	0.35	10	FRAG (saraf)
2	0.9	15	metak
2.75	0.15	10	PMA 2
4.2	0.45	10	PMA 3
4.8	0.7	20	FRAG
5.3	0.25	0-10	Ostatak tromblonske mine
5.7	0.8	15	FRAG
6	0.35	10	ITOP 10
6.7	0.6	20	Plasticcna plava kutija
7.2	0.35	20	FRAG (saraf)
9	0.45	20	FRAG
11.6	0.2	20	FRAG
12.7	0.15	10	Ostatak tromblonske mine
19.75	0.75	5	PMA 3
20.7	0.3	20	FRAG saraf)
21.1	0.85	20	Ostatak tromblonske mine
21.8	0.9	20	FRAG (saraf)
23.5	0.45	5	PMA 3

TABLE 4: Landmines: region-4-.

x(m)	y(m)	Debt(cm)	Type
0.6	0.25	10	PMA 2
1.9	0.55	10	PMA 2
2.3	0.8	15	PMA 2
3	0.3	15	FRAG
3.65	0.7	15	PMA 3
4.65	0.55	20	Ostatak tromblonske mine
5.65	0.55	15	PMA 2
8.3	0.15	20	Plasticna plava kutija
9	0.9	5	PMA 2
9..5	0.3	10	FRAG (saraf)
10.3	0.9	10	Bijeli surogat PMA 2
10.75	0.3	5	PMA 2
11.4	0.9	10	PMA 3
12.4	0.35	10	Ostatak tromblonske mine
13	0.7	15	PMA 3
13.8	0.9	20	Cahura metka
14.85	0.95	10	PMA 3
15.35	0.45	15	FRAG
18.8	0.75	10	CLUTTER
21.9	0.7	15	PMA 3
22.6	0.85	10	PMA 3
25	0.55	10	Ostatak tromblonske mine
27.2	0.3	10	Bijeli surogat PMA 2
27.2	0.9	10	Bijeli surogat PMA 2
27.6	0.3	10	Bijeli surogat PMA 2
27.6	0.9	10	Bijeli surogat PMA 2
28.4	0.3	10	Bijeli surogat PMA 2
28.4	0.9	5	Bijeli surogat PMA 2
28.9	0.3	10	Bijeli surogat PMA 2
28.9	0.9	20	Bijeli surogat PMA 2

TABLE 5: Landmines: region-5-.

x(cm)	y(cm)	Debt(cm)	meta
0.3	0.95	10	FRAG (saraf)
2.45	0.95	10	metak
3.25	0.25	15	FRAG (saraf)
3.7	0.35	20	Cahura metka
4.7	0.65	20	FRAG (saraf)
7.2	0.25	10	PMA 3
8.6	1	20	FRAG (saraf)
9	0.25	5	PMA 3
10	0.45	15	FRAG (saraf)
11.05	0.6	15	metak
11.55	0.7	5	FRAG (saraf)
12.1	0.25	10	PMA 3
13.25	0.35	10	puscano zrno
13.8	0.5	15	FRAG (saraf)
14.5	0.6	10	Ostatak tromblonske mine
15.5	0.3	20	CLUTTER
16.6	0.6	15	puscano zrno
17.8	0.55	15	FRAG (saraf)
18.85	0.45	5	PMA 3
19.25	0.2	10	PMA 3
19.9	0.65	15	FRAG (saraf)
23.3	0.65	15-20	Ostatak tromblonske mine
24.35	0.9	15	FRAG (saraf)
25.1	0.5	10	FRAG
25.9	0.7	5	PMA 2
27	0.9	15	FRAG (saraf)
24.4	0.3	10	FRAG

TABLE 6: Landmines: region-6-.

x(m)	y(m)	Debt(cm)	Type
2.3	0.95	15	ITOP 10
3.2	0.95	10	FRAG
4.3	0.85	15	Plasticcna plava kutija
5.4	0.45	10	Bijeli surogat PMA 2
6.3	0.35	10	PMA 2
6.3	1	10	FRAG
9.3	0.45	10	Bijeli surogat PMA 2
10	0.7	10	PMA 3
11.1	0.3	20	FRAG (saraf)
12	0.95	20	CLUTTER
13	0.9	10	Ostatak tromblonske mine
13.5	0.2	20	FRAG (saraf)
14.8	0.95	20	puscano zrno
15.35	0.6	15	FRAG
16.25	0.6	15	FRAG
16.85	0.85	15	puscano zrno
17.5	0.2	20	Bijeli surogat PMA 2
19.15	0.35	20	metak
19.9	0.95	10	ITOP 10
20.75	0.45	5	PMA 3
21.6	0.85	10	PMA 3
22.55	0.95	5	PMA 2
23	0.15	10	PMA 2
25	0.15	20	metak
25.2	0.7	15	Ostatak tromblonske mine
27.8	0.25	5	Bijeli surogat PMA 2
27.8	0.85	5	Bijeli surogat PMA 2
28.1	0.25	20	Bijeli surogat PMA 2
28.1	0.85	10	Bijeli surogat PMA 2

2.3 Use of vision-based remote sensor modalities at Benkovac test site

The Benkovac test site (https://www.ctro.hr/en/) was used in the International Test and Evaluation Programme (ITEP) project 2.1.1.2 "Reliability Model for Test and Evaluation of Metal Detectors" [6] in accordance with the European Committee for Standardization (CEN) workshop agreement (CWA) 14747 [38]. There are three types of soils available in different lanes in the Benkovac test site, namely neutral stones, red bauxite and neutral clay [6]. There are 8 test minefields designed for anti-personnel mine detectors as depicted in Fig. 6. The first 7 lanes starting from the right are

TABLE 7: Landmines: region-7-.

x(cm)	y(cm)	Debt(cm)	meta
0.1	0.3	15	ITOP 10
1.95	0.65	5	ITOP 10
3.55	0.55	10	FRAG (Saraf)
5.35	0.8	20	FRAG
7.75	0.8	10	ITOP 10
9.2	0.4	10	ITOP 10
10.1	0.85	20	FRAG
10.6	0.15	10	ITOP 10
11.7	0.6	20	CLUTTER
13.65	0.2	20	Metak 20mm
14.5	0.95	10	ITOP 10
19.9	0.15	20	Metak 7.62 mm

being actively used and different types of scattered mines were buried under variations of controlled variables.

Fig. 6: All test lanes: 1-8 from right to left.
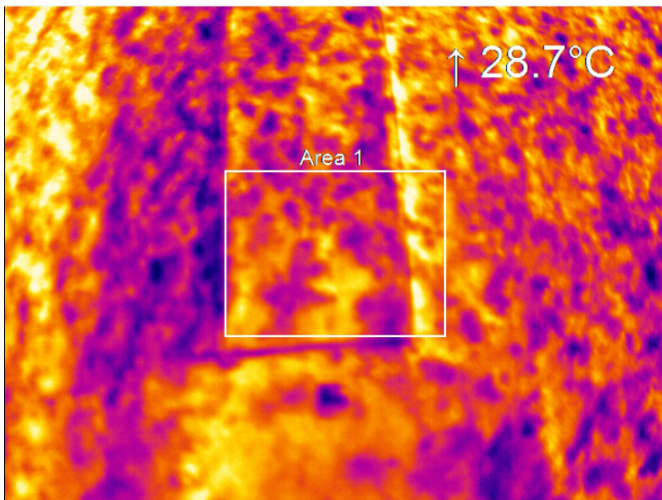
Fig. 7: An image from Optris PI 640 LWIR camera from lane-1.

3 SETUP

The data collection was conducted during mid-afternoon under clear skies with relative humidity of approximately 50% and temperatures varying from 25-27 °C. The flight altitude was set at about 3.5m at speeds of less than $0.3ms^{-1}$ aimed at extracting enough features from the ground to ensure the accurate detection of the scene and accurate geo-mapping of the terrain. There is a trade-off between the high and low flight altitude: the higher the flying altitude, the less time is needed for the generation of the map. To evaluate the feature confidence of the image mosaic (terrain map), we used a ground-truth image of the terrain to be mapped as shown in Figs. 8 and 9. In both figures, regarding the highlighted frames and registered lane-1 image, one can see that the mosaicking method was able to generate the corresponding map of the terrain accurately where the features of the panoramic images corresponded to those from the ground-truth image. Additionally, one can observe from the highlighted frames how the flight altitude changes the covered terrain areas with different altitude profiles.

3.1 Data collection

At a specifically prepared test field, different targets were buried at shallow depths in inhomogeneous soil. Each lane was analysed by the multispectral RGB camera mounted on the UAV. Several tests were conducted at these lanes. In each minefield, there are lanes with 1 m in width and 30 m in length. The video files and frames recorded by Multispectral RGB and LWIR cameras are in the supplementary materials for researchers who would like to develop techniques using the thermal datasets. A frame from the first lane captured by RGB camera mounted on the UAV is presented in Fig. 12. The channel components of 2nd frame of lane-1, namely green, nir, red and rededge, detected by the LWIR camera are shown in Fig. 10.

4 DISCUSSION AND CONCLUSION

When dealing with thermal modelling for landmine detection, one should keep in mind that LWIR signatures of the soil surface depend strongly on weather and environmental conditions and the soil type, in particular, the surface layer [20]. The presence of buried objects affects the heat conduction inside the soil under natural heating conditions and consequently, soil temperatures on the ground above the buried objects are often different from that of unperturbed areas [20]. Several factors affect the reflectance signature obtained by the imager: Wind and rain are the main factors, but the effect of rain is the dominant one [4]. In the case of buried landmines, rainfall decreases the reflected portion of the thermal energy and therefore the reflectance signal received [4]. Concerning these multiple changing parameters, the use of unsupervised ML clustering approaches to mitigate the dynamic features of landmine fields by using the intrinsic characteristics [39] seems to be an effective solution to be implemented.

This study concludes that no single mine sensor has the potential to increase the probability of detection and decrease FARs for all types of mines under the wide variety of environmental conditions in which mines exist; rather than

Fig. 8: Geo-mapping of 125 frames captured by the Multispectral Parrot SEQUOIA+ camera a larger terrain than the land fields starting from the biggest circle to the left and to the right using Pix4DMapper.

Fig. 9: Geo-mapping of 172 frames captured by the Multispectral Parrot SEQUOIA+ camera on the lane1 starting from the biggest red circle using Pix4DMapper.
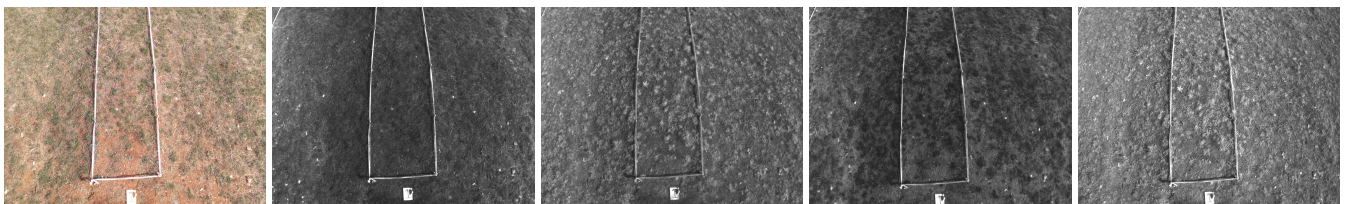

Fig. 10: 2nd frame of lane-1 detected by multi-spectral RGB camera (1st image) and its channel components (from left to right): green (2nd image), nir (3rd image), red (4th image) and rededge (5th image).
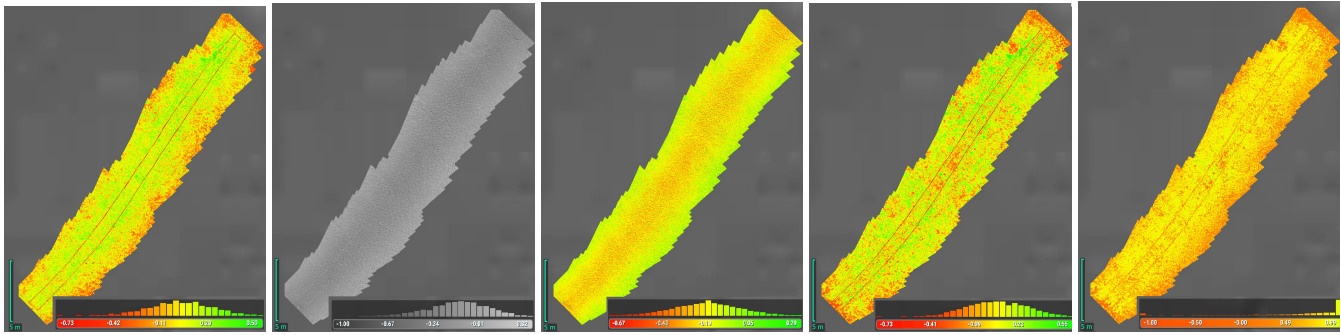
Fig. 11: Components of LWIR image of lane-1: GNDVI, LCI, NDRE, NDVI and SIPI2 from left to right.

Fig. 12: 2nd frame of lane-1 detected using RGB camera.

focusing on individual technologies operating in isolation, the design of an integrated, multisensory system that would overcome the limitations of any single-sensor technology would be a great development and the correct solution. Since a single detection technique will not be able to detect all types of landmines in various conditions, the fusion of data acquired from various techniques would increase the probability of the detection. Recent advances in cyber-physical systems (CPS) within the concepts of Internet of Everything (IoE) and Automation of Everything (AoE) [40] allow us to integrate smaller systems into a larger system. In this direction, we are incorporating a multiplicity of sensor modalities by fusing the data acquired from these sensors in our research, not just for detecting landmines but also for locating Unexploded Ordnance (UXO) [41], [42]. The vision-based remote sensing imagery datasets and the related knowledge based on a literature survey provided in this report aim to encourage researchers to develop bespoke efficient fusion techniques to detect landmine spots using multiple remote sensing modalities.

ACKNOWLEDGEMENT

guide us in the future development of the robots for mine detection and removal robots.

REFERENCES

[1] M. Ihab, "Hyperspectral imaging for landmine detection," Master's Thesis, Politecnico Di Torino, XXX, 2017.

[2] H. Aoyama, K. Ishikawa, J. Seki, M. Okamura, S. Ishimura, and Y. Satsumi, "Development of mine detection robot system," *International Journal of Advanced Robotic Systems*, vol. 4, no. 2, p. 25, 2007. [Online]. Available: https://doi.org/10.5772/5693

[3] S. B. i Badia, U. Bernardet, A. Guanella, P. Pyk, and P. F. Verschure, "A biologically based chemo-sensing uav for humanitarian demining," *International Journal of Advanced Robotic Systems*, vol. 4, no. 2, p. 21, 2007. [Online]. Available: https://doi.org/10.5772/5697

[4] I. Makki, R. Younes, C. Francis, T. Bianchi, and M. Zucchetti, "A survey of landmine detection using hyperspectral imaging," *ISPRS Journal of Photogrammetry and Remote Sensing*, vol. 124, pp. 40 – 53, 2017. [Online]. Available: http://www.sciencedirect.com/science/article/pii/S0924271616306451

[5] ICBL-CMC, "Landmine monitor 2015," International Campaign to Ban Landmines- Cluster Munition Coalition, Canada, , 2015.

[6] D. Guelle, M. Gaal, M. Bertovic, C. Mueller, M. Scharmach, and M. Pavlovic, "South-east europe interim report field trial croatia: Itep-project systematic test and evaluation of metal detectors - stemd," Federal Institute for Materials Research and Testing (BAM), Berlin, Germany, , 2007.

[7] C. Castiblanco, J. Rodriguez, I. Mondragón, C. Parra, and J. Colorado, *Air Drones for Explosive Landmines Detection*, 01 2014, vol. 253, pp. 107–114.

[8] X. Zhang, J. Bolton, and P. Gader, "A new learning method for continuous hidden markov models for subsurface landmine detection in ground penetrating radar," *IEEE Journal of Selected Topics in Applied Earth Observations and Remote Sensing*, vol. 7, no. 3, pp. 813–819, March 2014.

[9] C. P. Gooneratne, S. C. Mukhopahyay, and G. S. Gupta, "A review of sensing technologies for landmine detection: Unmanned vehicle based approach," pp. 401–407, December 2004.

[10] P. Gao and L. M. Collins, "A two-dimensional generalized likelihood ratio test for land mine and small unexploded ordnance detection," *Signal Processing*, vol. 80, no. 8, pp. 1669 – 1686, 2000. [Online]. Available: http://www.sciencedirect.com/science/article/pii/S0165168400001006

[11] J. Colorado, I. Mondragon, J. Rodriguez, and C. Castiblanco, "Geo-mapping and visual stitching to support landmine detection using a low-cost uav," *International Journal of Advanced Robotic Systems*, vol. 12, no. 9, p. 125, 2015. [Online]. Available: https://doi.org/10.5772/61236

[12] L. He, S. Ji, W. R. Scott, and L. Carin, "Adaptive multimodality sensing of landmines," *IEEE Transactions on Geoscience and Remote Sensing*, vol. 45, no. 6, pp. 1756–1774, June 2007.

[13] K. Kuru, D. Ansell, W. Khan, and H. Yetgin, "Analysis and optimization of unmanned aerial vehicle swarms in logistics: An intelligent delivery platform," *IEEE Access*, vol. 7, pp. 15 804–15 831, 2019.

[14] K. Kuru, "Planning the future of smart cities with swarms of fully autonomous unmanned aerial vehicles using a novel framework," *IEEE Access*, vol. 9, pp. 6571–6595, 2021.

[15] ——, "Conceptualisation of human-on-the-loop haptic teleoperation with fully autonomous self-driving vehicles in the urban environment," *IEEE Open Journal of Intelligent Transportation Systems*, vol. 2, pp. 448–469, 2021.

[16] K. Kuru, S. Worthington, D. Ansell, J. M. Pinder, A. Sujit, B. Jon Watkinson, K. Vinning, L. Moore, C. Gilbert, D. Jones *et al.*, "Aitl-wing-hitl: Telemanipulation of autonomous drones using digital twins of aerial traffic interfaced with wing," *IEEE Access*, vol. 11, 2023.

[17] K. Kuru, J. M. Pinder, B. J. Watkinson, D. Ansell, K. Vinning, L. Moore, C. Gilbert, A. Sujit, and D. Jones, "Toward mid-air collision-free trajectory for autonomous and pilot-controlled unmanned aerial vehicles," *IEEE Access*, vol. 11, pp. 100 323–100 342, 2023.

[18] K. Kuru, S. Clough, D. Ansell, J. McCarthy, and S. McGovern, "Intelligent airborne monitoring of irregularly shaped man-made marine objects using statistical machine learning techniques," *Ecological Informatics*, vol. 78, p. 102285, Dec. 2023. [Online]. Available: https://doi.org/10.1016/j.ecoinf.2023.102285

[19] ——, "WILDetect: An intelligent platform to perform airborne wildlife census automatically in the marine ecosystem using an ensemble of learning techniques and computer vision," *Expert Systems with Applications*, vol. 231, p. 120574, Nov. 2023. [Online]. Available: https://doi.org/10.1016/j.eswa.2023.120574

[20] N. T. Thanh, H. Sahli, and D. N. Hao, "Finite-difference methods and validity of a thermal model for landmine detection with soil property estimation," *IEEE Transactions on Geoscience and Remote Sensing*, vol. 45, no. 3, pp. 656–674, March 2007.

[21] A. Banerji and J. Goutsias, "A morphological approach to automatic mine detection problems," *IEEE Transactions on Aerospace and Electronic Systems*, vol. 34, no. 4, pp. 1085–1096, Oct 1998.

[22] J. M. M. Anderson, "A generalized likelihood ratio test for detecting land mines using multispectral images," *IEEE Geoscience and Remote Sensing Letters*, vol. 5, no. 3, pp. 547–551, July 2008.

[23] N. T. Thanh, H. Sahli, and D. N. Hao, "Infrared thermography for buried landmine detection: Inverse problem setting," *IEEE Transactions on Geoscience and Remote Sensing*, vol. 46, no. 12, pp. 3987–4004, Dec 2008.

[24] J. E. McFee, S. Achal, T. Ivanco, and C. Anger, "A short wave infrared hyperspectral imager for landmine detection," 2005. [Online]. Available: https://doi.org/10.1117/12.602637

[25] J. E. McFee, C. Anger, S. Achal, and T. Ivanco, "Landmine detection using passive hyperspectral imaging," 2007. [Online]. Available: https://doi.org/10.1117/12.722204

[26] J. M. Bioucas-Dias, A. Plaza, G. Camps-Valls, P. Scheunders, N. Nasrabadi, and J. Chanussot, "Hyperspectral remote sensing data analysis and future challenges," *IEEE Geoscience and Remote Sensing Magazine*, vol. 1, no. 2, pp. 6–36, June 2013.

[27] R. Younes, I. Makki, F. Clovis, and M. Zucchetti, "Mathematical methods for hyperspectral imaging in landmine detection," *Transactions of the American Nuclear Society*, vol. 112, pp. 420–423, 06 2015.

[28] A. Nikulin, T. de Smet, J. Baur, W. Frazer, and J. Abramowitz, "Detection and identification of remnant pfm-1 "butterfly mines" with a uav-based thermal-imaging protocol," *Remote Sensing*, vol. 10, no. 11, p. 1672, Oct 2018. [Online]. Available: http://dx.doi.org/10.3390/rs10111672

[29] J. Mcfee, S. Achal, T. Ivanco, and C. Anger, "A short wave infrared hyperspectral imager for landmine detection," *Proceedings of SPIE - The International Society for Optical Engineering*, 06 2005.

[30] M. T. Eismann, C. R. Schwartz, J. N. Cederquist, J. A. Hackwell, and R. J. Huppi, "Comparison of infrared imaging hyperspectral sensors for military target detection applications," 1996. [Online]. Available: https://doi.org/10.1117/12.258056

[31] J. S. Groot and Y. H. Janssen, "Remote land minefield detection. an overview of techniques," *Defense Technical Information Center: TNO Defence Research*, p. 52, 09 1994.

[32] E. M. Winter, M. A. Miller, C. G. Simi, A. B. Hill, T. J. Williams, D. Hampton, M. Wood, J. Zadnick, and M. D. Sviland, "Mine detection experiments using hyperspectral sensors," 2004. [Online]. Available: https://doi.org/10.1117/12.548087

[33] N. Playle, "Detection of landmines using hyperspectral imaging," 2006. [Online]. Available: https://doi.org/10.1117/12.664044

[34] D. Letalick, G. Tolt, S. Sjökvist, S. Nyberg, C. Grönwall, P. Andersson, A. Linderhed, G. Forssell, H. Larsson, and M. Uppsäll, "Multi-optical mine detection: results from a field trial - art. no. 62170d," *Proceedings of SPIE - The International Society for Optical Engineering*, vol. 6217, 05 2006.

[35] M.-A. Gagnon, P. Lagueux, J.-P. Gagnon, S. Savary, P. Tremblay, V. Farley, E. Guyot, and M. Chamberland, "Airborne thermal infrared hyperspectral imaging of buried objects," 2015. [Online]. Available: https://doi.org/10.1117/12.2177182

[36] T. S. de Smet and A. Nikulin, "Catching "butterflies" in the morning: A new methodology for rapid detection of aerially deployed plastic land mines from uavs," *The Leading Edge*, vol. 37, no. 5, pp. 367–371, 2018. [Online]. Available: https://doi.org/10.1190/tle37050367.1

[37] M. J. Khan, H. S. Khan, A. Yousaf, K. Khurshid, and A. Abbas, "Modern trends in hyperspectral image analysis: A review," *IEEE Access*, vol. 6, pp. 14 118–14 129, 2018.

[38] J. Ishikawa, K. Furuta, and N. Pavkovi, *Test and Evaluation of Japanese GPR-EMI Dual Sensor Systems at the Benkovac Test Site in Croatia*, bookTitle="*Anti-personnel Landmine Detection for Humanitarian Demining: The Current Situation and Future Direction for Japanese Research and Development*. London: Springer London, 2009, pp. 63–81. [Online]. Available: https://doi.org/10.1007/978-1-84882-346-4_5

[39] K. Kuru and W. Khan, "Novel hybrid object-based non-parametric clustering approach for grouping similar objects in specific visual domains," *Applied Soft Computing*, vol. 62, pp. 667–701, Jan. 2018. [Online]. Available: https://doi.org/10.1016/j.asoc.2017.11.007

[40] K. Kuru and H. Yetgin, "Transformation to advanced mechatronics systems within new industrial revolution: A novel framework in automation of everything (aoe)," *IEEE Access*, vol. 7, pp. 41 395–41 415, 2019.

[41] K. Kuru, D. Ansell, B. J. Watkinson, D. Jones, A. Sujit, J. M. Pinder, and C. Tinker-Mill, "Intelligent automated, rapid and safe landmine and unexploded ordnance (uxo) detection using multiple sensor modalities mounted on autonomous drones," *IEEE Transactions on Geoscience and Remote Sensing*, Sep. 2023. [Online]. Available: https://clok.uclan.ac.uk/49046/

[42] K. Kuru, A. Sujit, D. Ansell, B. J. Watkinson, D. Jones, J. M. Pinder, and C. Tinker-Mill, "Intelligent, automated, rapid and safe landmine and unexploded ordnance (uxo) detection using maggy," *IEEE Transactions on Geoscience and Remote Sensing*, Sep. 2023.

Kaya Kuru received the B.Sc. degree from National Defense University (Turkish Military Academy), the major/ADP degree in computer engineering from Middle East Technical University (METU), the M.B.A. degree from Selcuk University, the M.Sc. and Ph.D. degrees in computer science from METU. He completed his postdoctoral studies with the School of Electronics and Computer Science/Informatics, University of Southampton, UK. He is a Software Engineer and currently an Associate Professor of Computer-Information Systems Engineering. He has recently engaged in the implementation of numerous AI-based real-world systems within various funded projects. His research interests include the development of geo-distributed autonomous intelligent systems using FL, ML, DL, and DRL with CPSs.

Darren Ansell received the B.SC. from the University of Manchester Institute of Science and Technology in electrical and electronic engineer and Ph.D. from Cranfield University in antenna optimisation using evolutionary algorithms. He is the engineering lead for Space and Aerospace and Professor in Aerospace Engineering. He previously worked in industry at BAE Systems in management roles, specialising in Mission Systems and Autonomy.